# Multigram Scale Synthesis of Mechanically-Interlocked Derivatives of SWNT Using Green Mechanochemical Methods

Alicia Naranjo,[1] David M. Jiménez,[1] Marisol Rivas-Caramés,[1] Julia Villalva,[1] María Luisa Ruiz-González,[2] Henrik Pedersen,[3] Alejandro López-Moreno,[1] and Emilio M. Pérez[1*]

[1]IMDEA Nanociencia C/Faraday 9 Ciudad Universitaria de Cantoblanco, 28049 Madrid, Spain.

[2] Departamento de Química Inorgánica, Universidad Complutense de Madrid, 28040 Madrid, Spain

[3] Nanocore ApS, Langebjerg 1, 4000 Roskilde, Denmark

ABSTRACT: The grinding of chemical reagents enables mixing, promotes molecular collisions, and provides the thermal energy required for chemical reactions, while reducing the need for solvent (often to none) and significantly speeding up reactions. This has made mechanochemistry a powerful alternative to traditional solution chemistry. Here, we show that mechanically interlocked derivatives of single-walled carbon nanotubes (MINTs) can be made via mechanochemistry in multigram scale. Compared to the previously reported method in suspension, mechanochemistry allows us to reduce the amount of solvent by two orders of magnitude and the reaction time from 72 h to 5 min. The mechanochemical synthesis of MINTs is proven to work both with purified (6,5)-SWNTs and affordable Tuball™ SWNTs, enabling the cheap, fast, and environmentally friendly multigram scale synthesis of MINTs. With this new synthetic methodology we open the door to the real-world applications of MINTs in fields such as polymer composites.

Chemical derivatization of single-walled carbon nanotubes (SWNTs) is often required to make the most of their outstanding physical properties.[1-5] Covalent or supramolecular chemistry approaches have represented the bulk of the work in this area, each with its own advantages and disadvantages. Covalent

chemistry provides very robust hybrids but implies saturation of the C $sp^2$ network of the SWNTs, which in principle is not desirable.[6-8] Meanwhile, supramolecular chemistry is intrinsically dynamic, so the attachment between the SWNT and the molecular fragments depends on the conditions.[9-10] In the last few years, the chemistry of the mechanical bond has been successfully implemented for SWNTs.[11] Basically, macrocyclic species encapsulate the SWNTs forming rotaxane-type mechanically-interlocked SWNT [12]. Several synthetic pathways towards MINTs have been developed. We have developed a clipping strategy in which U-Shaped molecules first associate SWNTs and then are closed around them using ring-closing metathesis (RCM).[13] Meanwhile, Miki *et al.* used a threading strategy with preformed rigid macrocycles.[14] Von Delius et al. have explored the formation of 1+1 macrocyclic species around the SWNTs using self-correcting S-S chemistry.[15] Finally, noncovalent bonds, such as metal-ligand coordination[16-17] or H-bonding[18] can also be used to close the macrocyclic species around the SWNTs. Derivatization of SWNTs to form MINTs has shown to be potentially useful in several fields, including catalysis,[19-21] spintronics,[22] or the reinforcement of polymers.[23-30] But there is still a major hurdle to overcome for MINTs to become a relevant enabling technology: the lack of a scalable synthetic method. For example, our standard protocol[11] uses prohibitively expensive chirality-enriched SWNTs, involves the use of large amounts of solvent, and takes 24-72 hours to reach full functionalization of the SWNTs, to finally afford milligram quantities of MINTs.[31]

Mechanochemistry has emerged as a powerful alternative to traditional solution-based chemistry.[32-33] Conceptually, it is based on applying mechanical energy both to enable collisions and thermally activate the reagents, fulfilling the functions of solvent (stirring) and heat. It therefore does not present any intrinsic limitations in scope in terms of structure of the reagents or types of reaction. Accordingly, it has been successfully applied to many different types of reactions, including those most relevant to the

objectives of this work: ring-closing metathesis,[34] derivatization of SWNTs,[35] and formation of mechanically interlocked species.[36-39]

Here, we describe the multigram-scale synthesis of MINTs using mechanochemistry. Our protocol uses standard ball-milling equipment, is quick (minutes) and uses minimal amounts of solvent for the synthesis and small amounts for the purification. It applies to both small diameter (6,5)-SWNTs and affordable mixtures of SWNTs of large diameter, therefore meeting all the requirements for further scalability.

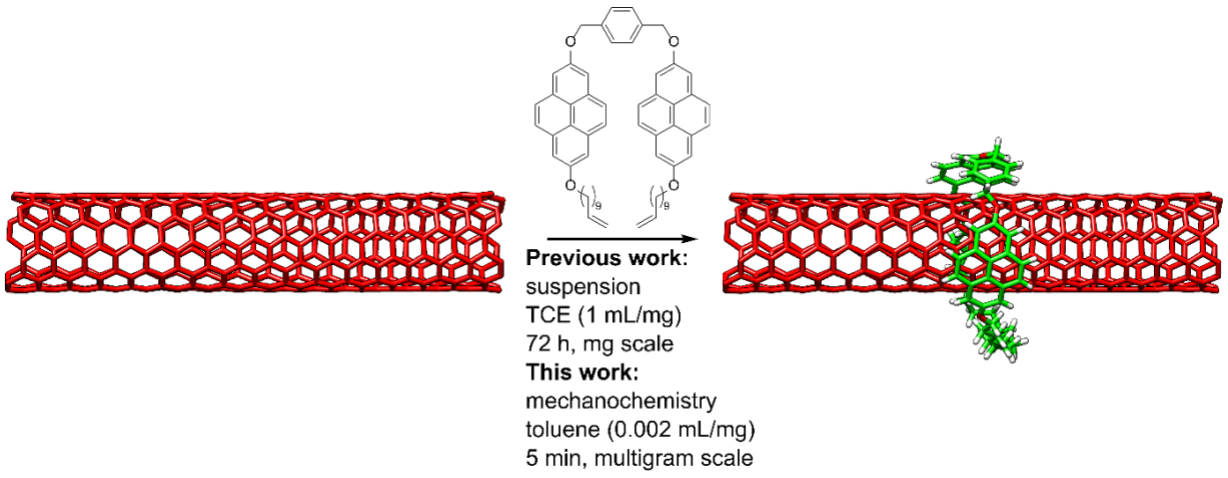


**Figure 1**. Synthesis of MINTs in suspension and by mechanochemistry.

To test the potential of mechanochemistry to synthesize MINTs, we focused on a pyrene-based U-Shape precursor (pyr-U-shape, Figure 1), which is synthetically accessible in multigram scale. We have previously used that same U-Shape to make MINTs based on (6,5) and (7,6)-enriched SWNTs,[40] and have recently shown that it can also form MINTs using cheaper mixtures of SWNTs, thanks to the possibility of forming rings of different stoichiometries (predominantly 1+1)[15] to encapsulate SWNTs of larger diameter.[41] As a preliminary test, we mixed SWNTs ((6,5)-SWNTs, 25 mg, 0.784 nm diameter), pyr-U-Shape (22 mg, 0.025 mmol) and Grubbs' 2$^{nd}$ generation catalyst (22 mg, 0.025 mmol),

using the same ratio we typically employ in suspension, and ground the mixture manually using an agate mortar and pestle for 30 minutes. As a control sample, we mixed the same amounts of SWNTs and U-Shape and ground them in the absence of Grubbs' catalyst. The powders obtained in each case were washed three times with $CH_2Cl_2$ (3x50 mL) with 5 min sonication at each wash. After the last wash, the samples were filtered and subjected to thermogravimetric analysis (TGA). The TGA results are shown in Figure S1a, together with a reference sample of MINTs made in suspension using the same molecular components. We were happy to see that the TGA traces of the sample synthesized in suspension and the one made by mechanochemistry showed similar content of organic material. In particular, there is only one significant weight loss due to the added organic material, centred at approximately 400 ºC, and the degree of functionalization is in both cases around 28-30 %. These features indicate the formation of MINTs without significant participation of supramolecularly attached oligomers, which can be easily identified by TGA.[31] In comparison, the control sample that was ground in the absence of Grubbs' catalyst showed very little functionalization due to unwashed physisorbed U-Shape (< 5 %, consistent with control experiments in suspension). The Raman spectra ($\lambda_{exc}$ = 532 nm) of the samples synthesized in suspension and by hand-grinding also show similar trends with respect to the pristine SWNTs, as shown in Figure S1b. In particular, the relative intensity of the D-band was only slightly affected after functionalization in the case of the mechanochemical synthesis, showing a quantitatively very small but noticeable degree of damage of the SWNTs subjected to the ball-milling procedure (from $I_D/I_G$ = 0.018 ± 0.002 to 0.030 ± 0.005). This is comparable to the change observed for the MINTs synthesized in suspension, and therefore most likely originated in the sonication steps during the purification procedures. In both cases, the minute change in $I_D/I_G$ supports the formation of noncovalent derivatives, as a much larger increase in $I_D/I_G$ would be expected for a covalent derivative with similar degree of functionalization.[42] We also observed slight differences in the radial breathing modes (RBM). The RBM at 271±1 $cm^{-1}$ (diameter of 0.91 nm) presents no significant differences with respect to pristine (6,5)-

SWNTs and MINTs$_{65}$ prepared in TCE. On the other hand, RBM band at 311±1 cm$^{-1}$ (diameter of 0.8 nm) showed a slight increase in intensity with respect of the pristine nanotubes and MINTs prepared in TCE. Finally, we do not notice significant changes in the G or 2D bands, indicating that the SWNTs show very little or no doping upon chemical modification. Again, these results are consistent compared with the sample prepared by the suspension method. As we reported for (6,5)-SWNTs with different macrocycles, [13, 40], we decided to investigate if we could modulate the functionalization in commercially available using mechanochemistry. We used four different amounts of U-shape with respect the SWNTs (0.12, 0.24, 0.48 and 1 μmmol/mg$_{SWNTs}$). The product formed by hand milling with the lowest concentration of U-shape showed a loss of 12 % whereas weight losses of 21, 28 and 35 % were observed when the concentration increased (Figure S3).

With these encouraging results, we tested the formation of MINTs using a commercially available planetary ball-mill equipped with stainless steel reactors and balls. After each milling experiment, the resulting powder was collected and the unreacted U-Shapes, and Grubbs' catalyst were removed by three washes in DCM, in which we suspend the product in 20 mL of DCM with 5 minutes bath sonication and then filter the solid through a 0.2 μm pore PTFE membrane. We used 20 mL reactors and 50 mg of (6,5)-SWNTs, 21 mg of U-Shape (0.48 μmol/mg) and 10.2 mg of Grubbs' catalyst (0.5 eq. with respect to U-Shape) to optimize the number of steel balls and the time required to obtain a functionalization degree similar to that obtained in suspension and by hand-grinding. We carried out experiments at 150 and 500 rpm for five minutes with different numbers of steel balls finding that optimal conditions to obtain comparable results to solution and hand-grinding methods were 2 steel balls, five minutes grinding at 150 rpm and a small amount of toluene (0.4 mL), with which we obtained a satisfactory 28 % functionalization with a decomposition temperature centred at 400 ºC, matching with suspension MINTs (Figure 2a). To test the extent of physisorbed organic material that remains even after the three DCM

washes, we dispersed the sample in tetrachloroethane (TCE), in which the U-Shape and its derivatives are highly soluble, and refluxed it (b.p. 147 ºC) for one hour. After this, the sample was filtered and washed again three times with DCM, following the procedure described above, and once with diethyl ether ($Et_2O$) to remove traces of DCM and facilitate drying. The sample was further dried in an oven (T = 110 ºC) overnight to remove any solvent residues (absorbed or encapsulated). The TGA data from this sample (Figure S2) shows that only a small fraction of the organic material (ca. 5 %) is removed after this exhaustive washing procedure, a characteristic of the formation of MINTs.[11]

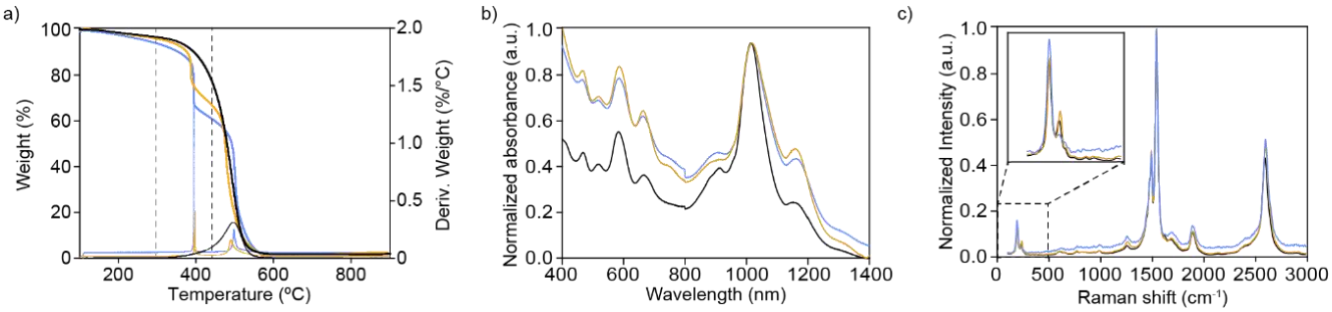


**Figure 2.** a) TGA (Air, 10 ºC·min$^{-1}$) of (6,5)-SWNTs (black), MINTs$_{(6,5)}$ synthesized in TCE (blue), MINTs$_{(6,5)}$ synthesized by mechanochemistry using: 150 rpm, 2 balls, 5 min and 0.4 mL of toluene (yellow); b) UV/Vis/NIR spectra ($D_2O$, 1 % sodium dodecyl sulfate (SDS), 298 K) of (6,5)-SWNTs (black); MINTs$_{(6,5)}$ synthesized in TCE (blue) and MINTs$_{(6,5)}$ synthesized by mechanochemistry using 150 rpm, 2 ball, 5 min and 0.4 mL of toluene (yellow); c) Raman spectra with RBM region zoom ($\lambda_{exc}$ = 633 nm) of (6,5)-SWNTs (black); MINTs$_{(6,5)}$ synthesized in TCE (blue); and MINTs$_{(6,5)}$ synthesized by mechanochemistry using 150 rpm, 2 ball, 5 min and 0.4 mL of toluene (yellow).

UV/Vis/NIR extinction spectra of MINTs prepared by both suspension and ball-mill methods and pristine (6,5)-SWNTs as reference, all taken in $D_2O$ with 1 % sodium dodecyl sulfate (SDS) at room temperature, are shown in Figure 2b. With respect to pristine (6,5)-SWNTs, we observe a shift of the $E_{11}$ and $E_{22}$ interband transitions, from 1014 to 1019 nm and from 584 to 586 nm, respectively, in the

mechanochemically synthesized MINT samples. The sample synthesized in suspension shows qualitatively and quantitatively identical changes, indicating that both strategies lead to the same type of product. The Raman characterization of the samples synthesized under optimal conditions again exhibited trends that perfectly mirror those observed for MINTs formed in suspension with respect to the pristine (6,5)-SWNTs (Figure 2c). Detailed statistical analyses of peak position and intensity ratios are provided in the Supporting Information section (Figure S4-S6). In particular, the D (ca. 1300 $cm^{-1}$), $G^-$ (ca. 1535 $cm^{-1}$), and $G^+$ (1590 $cm^{-1}$) bands demonstrated no significant shifts post-functionalization, in agreement with the suspension method results. Regarding the radial breathing modes (RBM, 250–350 $cm^{-1}$; zoom in Figure 2c), we also observed similar variations in Raman shift and relative intensity beetween ball-milling and suspension MINTs compared to pristine SWNTs. For excitation at λexc = 532 nm (Figure 2c), we observe two main RBM peaks for pristine SWNTs at 269 ± 2 $cm^{-1}$, which corresponds to a diameter of 0.92 nm and 309 ± 3 $cm^{-1}$ (diameter of 0.80 nm). Upon formation of MINTs, no significant shift or change of the intensity of the bands were found. Photoluminescence excitation (PLE) maps of the (6,5)-enriched SWNTs show an intense peak at $\lambda_{exc}$ = 565 nm, $\lambda_{em}$ = 985 nm characteristic of the (6,5) chirality, which is 99 % quenched upon functionalization using both solution and mechanochemistry methods (Figure S7). From all these data, including control experiments, TGA, UV/Vis/NIR, Raman and PLE, we interpret that the mechanochemically synthesized product are indeed MINTs.

In order to demonstrate the scalability of the method, we carried out the preparation of MINT using the optimal conditions (150 rpm, 2 ball, 5 min, 0.4 mL of toluene) with affordable mixtures of SWNTs of large diameter using Tuball$^{TM}$ SWNTs (1.6 ±0.4 nm diameter), for which we have already proven the formation of MINTs in suspension.[41] For the mechanochemical method, we use 1 g of SWNTs, 420 mg of U-Shape (0.48 µmol/mg) and 204 mg of Grubbs' catalyst (0.5 µmol/ U-Shape µmol) and 2 mL of

Toluene. The functionalization of $MINT_{TUBALL}$ (around 22%) matches with the solvent method MINTs (around 28 %) corroborated with the TGA performed in air (Figure 3a). UV/Vis/NIRextinction spectra ($D_2O$ with 1 % sodium dodecyl sulfate (SDS) at room temperature) of MINTs prepared by both suspension and ball-mill methods and pristine SWNTs are shown in Figure 3b. No significant differences are observed between both MINTs samples, indicating that both strategies are equally valid for the preparation of MINTs. For instance, both show equivalent red shifts of the $S_{22}$ and the $S_{11}$ interband absorptions, at 680 - 800 nm and 900 - 1200 nm, respectively (see inset in Figure 3b). We have typically found these red shifts upon derivatization of SWNTs as MINTs[43] with macrocycles featuring pyrene units.[40] Interestingly, the spectra in the 900 - 1000 nm region show better defined interband absorptions for MINT samples with respect to pristine SWNTs, which is typically a sign of better individualization.[44]

The Raman characterization of $MINT_{TUBALL}$ exhibited trends that resembled those observed for MINTs formed in suspension and the pristine SWNTs, (Figure 3c). Detailed statistical analyses of peak position and intensity ratios are provided in the Supporting Information section (Figure S8-S10) The D, $G^-$, and $G^+$ bands demonstrated no significant shifts post-functionalization, in agreement with the suspension method results. Under optimal ball-milling conditions, we found that $I_D/I_G$ presented no significant changes with respect of those found for MINTs prepared by suspension method (Figure S8-S10). Regarding radial breathing modes (Figure 3c and S8-S10), we also observed similar variations in Raman shift and relative intensity of the ball-milling and suspension MINTs compared to pristine SWNTs. For excitation at $\lambda_{exc}$ = 633 nm (Figure 3c), we observe a main RBM peak for pristine SWNTs at 145.8 ± 0.8 $cm^{-1}$, which corresponds to a diameter of 1.7 nm, with shoulders at 163 ± 1 $cm^{-1}$ and 181 ± 2 $cm^{-1}$. Upon formation of MINTs, we note an obvious change in the relative intensities of these signals, with the higher frequency peak becoming significantly more intense. We also note shifts to higher frequencies of

the two most prominent RBMs, from 145.8 ± 0.8 $cm^{-1}$ (SWNTs) to 152.7 ± 0.6 $cm^{-1}$ (suspension MINTs), and 148 ± 2 $cm^{-1}$ (ball-milled MINTs). This shift follows the same trend and is quantitatively similar for the higher frequency RBM, from 181 ± 2 $cm^{-1}$ (SWNTs) to 189 ± 2 $cm^{-1}$ (suspension MINTs), and 189 ± 1 $cm^{-1}$ (ball-milled MINTs). From these data, we interpret that suspension MINTs and both mechanochemically synthesized MINTs (using (6,5)-SWNTs or Tuball™) share the same type of functionalization, in agreement with the TGA and absorption data. The changes in relative intensities between the RBMs corresponding to the larger diameter SWNTs (ca. 1.7 nm) compared to the smaller ones (ca. 1.3 nm) also point to some degree of diameter selectivity. Similar shifts to higher frequencies are also observed in the RBMs with 532 and 785 nm excitations (see the SI Figures S4-S6 and S8-S10 for (6,5)-SWNTs and Tuball™ respectively), and are indicative of a hardening of the radial vibrations of the SWNTs,[45] which is a reasonable consequence of surrounding their structure with macrocycles.

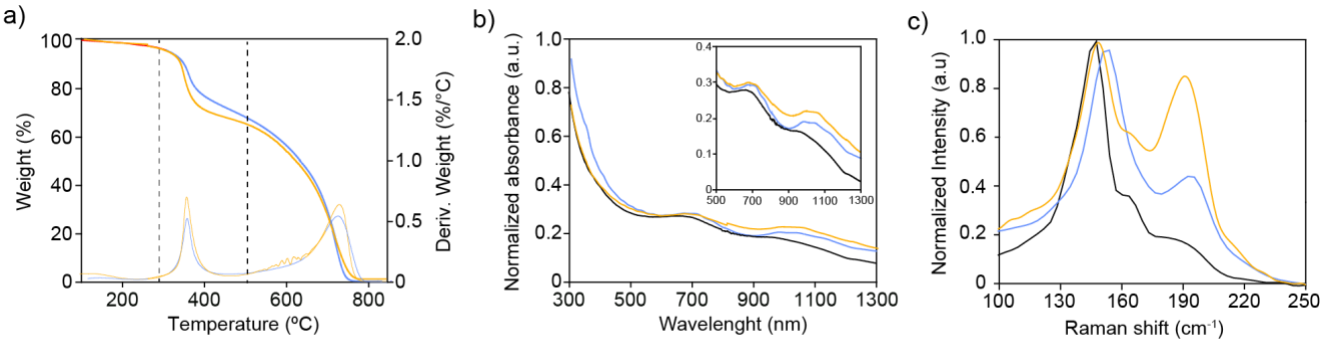


**Figure 3.** a) TGA (Air, 10 ºC·$min^{-1}$) of $MINT_{TUBALL}$ synthesized in TCE (blue) and $MINT_{TUBALL}$ synthesized by mechanochemistry using 150 rpm, 2 ball, 5 min and 2 mL of toluene (yellow); b) UV/Vis/NIR spectra ($D_2O$, 1 % sodium dodecyl sulfate (SDS), 298 K) of SWNTs (black); $MINT_{TUBALL}$ synthesized in TCE (blue) and $MINT_{TUBALL}$ synthesized by mechanochemistry using 150 rpm, 2 ball, 5 min and 2 mL of toluene (yellow); c) RBM region zoom ($\lambda_{exc}$ = 633 nm) of SWNTs (black); $MINT_{TUBALL}$

synthesized in TCE (blue); and $MINT_{TUBALL}$ synthesized by mechanochemistry using 150 rpm, 2 ball, 5 min and 2 mL of toluene (yellow).

Finally, microscopic analysis under AFM and TEM of the $MINT_{(6,5)}$ and $MINT_{TUBALL}$ synthesized using the ball-mill under optimal conditions also shows results consistent with our previous observations for MINTs synthesized with the suspension method. Figures 5a and 5c show AFM micrographs of the ball-milled MINTs. For $MINTs_{(6,5)}$ Figure 4a-b shows a topographic image of a single SWNT with a height of roughly 1 nm, on which three elevations of approximately 2.0 – 2.2 nm are observed. For $MINT_{TUBALL}$ sample we observe individual SWNTs (diameter ca. 1.6 nm as measured in the clean areas), almost entirely covered with a uniform coating of around 3 nm (Figure 4c-d). These are the same type of structures that we encountered in the MINTs synthesized with the suspension method with the same SWNTs and the same U-Shape molecule.[41] Aberration corrected HR-TEM analysis (60 kV) of samples of $MINT_{(6,5)}$ (Figure 4e) and $MINT_{TUBALL}$ (Figure 4g) drop casted from a TCE suspension shows mostly bundled nanotubes with heavily functionalized sidewalls, in agreement with the TGA data. Within these samples, the individualized tubes contain organic fragments whose size and shape are consistent with macrocycles. For example, in Figure 4e we observe a macrocycle clearly placed around the SWNT, and the remains of another macrocycle that decomposed during e-beam irradiation. In the case of $MINT_{TUBALL}$ we find similar structures although the macrocycles found are approximately twice the size (Figure 4g), in accordance with the majority 1+1 stoichiometry.[41] Interestingly, we found that after the ball-milling process, in addition to the formation of macrocycles, the encapsulation of organic material in the larger diameter tubes took place (Figure 4g and Figure S11). To evaluate the functionalization of the nanotubes, we measured the intertube distance between carbon nanotubes in the bundles. This measurement serves as an estimation of the lower bounds of intertube distance, as in most cases, the nanotubes are observed in van der Waals contact (d = 0). For $MINT_{(6,5)}$ this average intertube distance

of 0.11 ± 0.06 nm (N=50) is significantly larger than that of pristine SWNT bundles, as determined by HRTEM (0.06 ± 0.06 nm, N=50), suggesting a de-bundling effect due to high functionalization.[46] Same trend was found for Tuball samples where the average intertube distance of MINT is 0.16 ± 0.03 nm (N=50), larger than Tuball SWNTs (0.10 ± 0.03 nm (N=50).

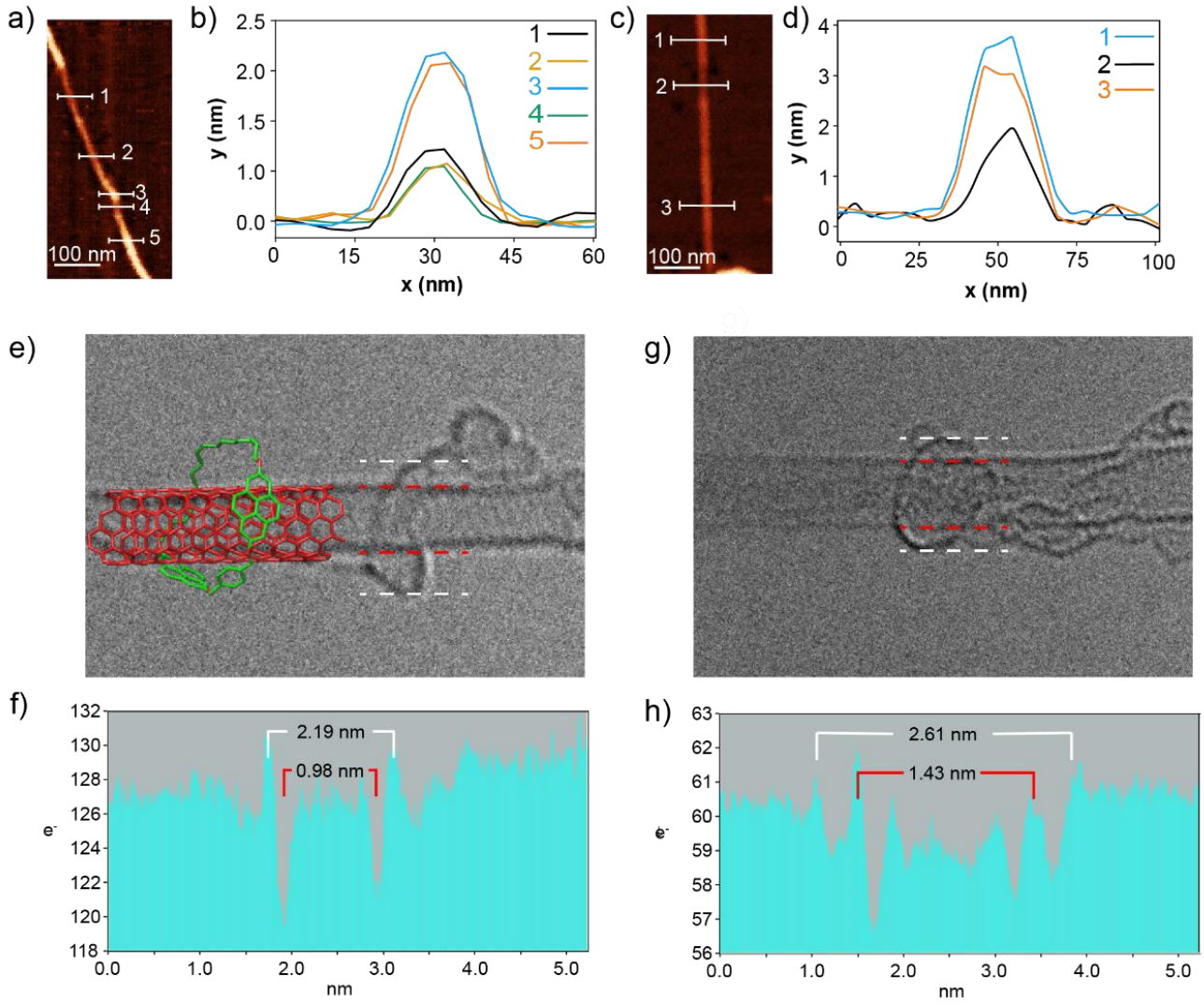


**Figure 4.** a) AFM topographic image of $MINT_{(6,5)}$ synthesized by mechanochemistry using 150 rpm, 2 ball, 5 min and 2 mL of toluene; b) height profiles along the lines marked in the topographic image a); c) AFM topographic image of a suspension in TCE of $MINT_{TUBALL}$ synthesized by mechanochemistry using 150 rpm, 2 ball, 5 min and 2 mL of toluene; d) height profiles along the lines marked in the

topographic image c); e) ac-HRTEM image of $MINT_{(6,5)}$ synthesized by mechanochemistry using 150 rpm, 2 ball, 5 min and 2 mL of toluene; f) profile graph of e), showing the dimensions of the SWNT and the macrocycle; g) ac-HRTEM image of $MINT_{TUBALL}$ synthesized by mechanochemistry using 150 rpm, 2 ball, 5 min and 2 mL of toluene; and h) profile graph of e), showing the dimensions of the SWNT and the macrocycle.

## Conclusion

In summary, we disclose that MINTs can be synthesized in multigram scale using environmentally friendly mechanochemistry. The mechanochemical method works well for both thin (6,5)-SWNTs which are expected to form MINTs via direct RCM of the U-Shape, and for thicker and cheap Tuball SWNTs, in which a mix of stoichiometries, dominated by 1+1 macrocycles are present. Full characterization of $MINT_{(6,5)}$ and $MINT_{TUBALL}$ corroborate that the products are identical to those obtained in suspension, with the exception of the thicker (radius > 1.8 nm) species in the Tuball SWNTs, for which HRTEM analysis shows organic fragments both around them, forming MINTs, and encapsulated within them. Compared to the previously reported method in suspension, mechanochemistry allows to reduce the amount of solvent by three orders of magnitude (from 1 mL/mg to 0.002 mL/mg), the reaction time from 72 h to 5 min, and the purification time from 12 h to 30 min. All these improvements together make the synthesis of MINTs in multigram scale economically viable, enabling their applications in real world technologies, like the reinforcement of polymers.

## Acknowledgements

This research was carried out with funding from Nanocore ApS (Copenhagen, Denmark). The authors would also like to acknowledge funding from the European Research Council (PoC-842606-PINT) the

Ministerio de Ciencia e Innovación (PID2020-116661RB-I00 and PID2023-152267NB-I00) and the Comunidad de Madrid (PR47/21 MAD2D-CM PRTR-CM). IMDEA Nanociencia receives support from the "Severo Ochoa" Programme for Centres of Excellence in R&D (MICINN, Grant CEX2020-001039-S)

## Competing Interests statement

The potential commercial applications of this research are protected by several patents and patent applications, all property of Nanocore ApS.

## References

[1] N. Karousis, N. Tagmatarchis, D. Tasis, *Chem. Rev.* **2010**, *110*, 5366-5397.
[2] Z. Liu, S. Tabakman, K. Welsher, H. Dai, *Nano Res.* **2009**, *2*, 85-120.
[3] Z. Spitalsky, D. Tasis, K. Papagelis, C. Galiotis, *Prog. Polym. Sci.* **2010**, *35*, 357-401.
[4] M. F. L. De Volder, S. H. Tawfick, R. H. Baughman, A. J. Hart, *Science* **2013**, *339*, 535-539.
[5] V. Schroeder, S. Savagatrup, M. He, S. Lin, T. M. Swager, *Chem. Rev.* **2019**, *119*, 599-663.
[6] A. Hirsch, *Angew. Chem. Int. Ed.* **2002**, *41*, 1853-1859.
[7] N. Karousis, N. Tagmatarchis, D. Tasis, *Chem. Rev.* **2010**, *110*, 5366-5397.
[8] P. Singh, S. Campidelli, S. Giordani, D. Bonifazi, A. Bianco, M. Prato, *Chem. Soc. Rev.* **2009**, *38*, 2214-2230.
[9] Y.-L. Zhao, J. F. Stoddart, *Acc. Chem. Res.* **2009**, *42*, 1161-1171.
[10] E. M. Pérez, N. Martín, *Chem. Soc. Rev.* **2015**, *44*, 6425-6433.
[11] A. López-Moreno, J. Villalva, E. M. Pérez, *Chem. Soc. Rev.* **2022**, *51*, 9433-9444.
[12] S. R. Adams, J. P. Y. Kao, G. Grynkiewicz, A. Minta, R. Y. Tsien, *J. Am. Chem. Soc.* **1988**, *110*, 3212-3220.
[13] A. de Juan, Y. Pouillon, L. Ruiz-González, A. Torres-Pardo, S. Casado, N. Martín, A. Rubio, E. M. Pérez, *Angew. Chem., Int. Ed.* **2014**, *53*, 5394-5400.
[14] K. Miki, K. Saiki, T. Umeyama, J. Baek, T. Noda, H. Imahori, Y. Sato, K. Suenaga, K. Ohe, *Small* **2018**, *14*, 1800720.
[15] B. Balakrishna, A. Menon, K. Cao, S. Gsänger, S. B. Beil, J. Villalva, O. Shyshov, O. Martin, A. Hirsch, B. Meyer, U. Kaiser, D. M. Guldi, M. von Delius, *Angew. Chem. Int. Ed.* **2020**, *59*, 18774-18785.
[16] A. López-Moreno, S. Ibáñez, S. Moreno-Da Silva, L. Ruiz-González, N. Martín Sabanés, E. Peris, E. M. Pérez, *Angew. Chem. Int. Ed.* **2022**, *61*, e202208189.
[17] G. Cheng, T. Hayashi, Y. Miyake, T. Sato, H. Tabata, M. Katayama, N. Komatsu, *ACS Nano* **2022,** *16*, 12500–12510.

[18] R. Chamorro, L. de Juan-Fernández, B. Nieto-Ortega, M. J. Mayoral, S. Casado, L. Ruiz-González, E. M. Pérez, D. González-Rodríguez, *Chem. Sci.* **2018**, *9*, 4176-4184.
[19] M. Blanco, B. Nieto-Ortega, A. d. Juan, M. Vera-Hidalgo, A. López-Moreno, S. Casado, L. R. González, H. Sawada, J. M. González-Calbet, E. M. Pérez, *Nat. Comm.* **2018**, *9*, 2671.
[20] D. Wielend, M. Vera-Hidalgo, H. Seelajaroen, N. S. Sariciftci, E. M. Perez, D. R. Whang, *ACS Appl. Mater. Interfaces* **2020**, *12*, 32615–32621.
[21] W. Zhang, M. Guillén-Soler, S. Moreno-Da Silva, A. López-Moreno, L. R. González, M. d. C. Giménez-López, E. M. Pérez, *Chem. Sci.* **2022**, *13*, 9706-9712.
[22] S. Moreno-Da Silva, J. I. Martínez, A. Develioglu, B. Nieto-Ortega, L. de Juan-Fernández, L. Ruiz-González, A. Picón, S. Oberli, P. J. Alonso, D. Moonshiram, E. M. Pérez, E. Burzurí, *J. Am. Chem. Soc.* **2021**, *143*, 21286-21293.
[23] A. López-Moreno, B. Nieto-Ortega, M. Moffa, A. de Juan, M. M. Bernal, J. P. Fernández-Blázquez, J. J. Vilatela, D. Pisignano, E. M. Pérez, *ACS Nano* **2016**, *10*, 8012-8018.
[24] M. Lundorf, H. Pedersen, T. Dehli, Designof composite materials with desired characteristics, US11028240, **2015.**
[25] H. Pedersen, M. D. Lundorf, T. Dehli,C. B. O. Nielsen, Composite Materials Comprising Mechanical Ligands, EP3737711, **2018**
[26] H. Mena, Sofía, E. M. Pérez, W. Xu, W. Zhang, Pedersen, Henrik, M. D. Lundorf, A. López-Moreno, Electrospinning of carbon nanotube composites, PCT/EP2022/067756, **2021**.
[27] H. Pedersen, M. González, A. López-Moreno, J. Villalva, M. d. L. González-Juarez, M. D. Eaton, E. M. Pérez, M. D. Lundorf, I. Isasti, S. Miranda-Alcazar, M. Rivas-Caramés, A. Naranjo, W. Zhang, W. Xu, S. Mena-Hernando, Industrial use of the Lasso principle for carbon nanotube composite production, PCT/EP2022/067728, **2021**.
[28] A. Rapakousiou, E. M. Pérez, H. Pedersen, M. D. Lundorf, J. Villalva, Ring-opening metathesis reactions for preparation of carbon nanotube composites. PCT/EP2022/067741, **2021**.
[29] M. González-Sánchez, H. Pedersen, A. López-Moreno, J. Villalva, M. D. Eaton, M. d. L. González-Juárez, E. M. Pérez, I. Isasti, S. Miranda-Alcázar, M. Rivas-Caramés, A. Naranjo-Chacón, M. D. Lundorf, Repairable and conductive nanocomposites, in situ polymerization and mechanochemistry, EP23382038.0, **2022**.
[30] J. Villalva, H. Pedersen, A. López-Moreno, M. González, E. M. Pérez, J. González, M. d. Lourdes, M. Rivas-Caramés, M. D. Eaton, I. Isasti, S. Miranda, M. D. Lundorf, A. Naranjo, Composite materials and processes for the preparation thereof, WO2024002950A1, **2024**.
[31] A. de Juan, M. Mar Bernal, E. M. Pérez, *ChemPlusChem* **2015**, *80*, 1153-1157.
[32] T. Friščić, C. Mottillo, H. M. Titi, *Angew. Chem. Int. Ed.* **2020**, *59*, 1018-1029.
[33] S. L. James, C. J. Adams, C. Bolm, D. Braga, P. Collier, T. Friic, F. Grepioni, K. D. M. Harris, G. Hyett, W. Jones, A. Krebs, J. MacK, L. Maini, A. G. Orpen, I. P. Parkin, W. C. Shearouse, J. W. Steed, D. C. Waddell, *Chem. Soc. Rev.* **2012**, *41*, 413 - 447.
[34] J.-L. Do, C. Mottillo, D. Tan, V. Štrukil, T. Friščić, *J. Am. Chem. Soc.* **2015**, *137*, 2476-2479.
[35] N. Rubio, C. Fabbro, M. A. Herrero, A. de la Hoz, M. Meneghetti, J. L. G. Fierro, M. Prato, E. Vázquez, *Small* **2011**, *7*, 665-674.
[36] T.-w. Kwon, B. Song, K. W. Nam, J. F. Stoddart, *J. Am. Chem. Soc.* **2022**, *144*, 12595-12601.
[37] M. Holler, T. Stoerkler, A. Louis, F. Fischer, J.-F. Nierengarten, *Eur. J. Org. Chem.* **2019**, *2019*, 3401-3405.
[38] A. Orita, J. Okano, Y. Tawa, L. Jiang, J. Otera, *Angew. Chem. Int. Ed.* **2004**, *43*, 3724-3728.
[39] S.-Y. Hsueh, K.-W. Cheng, C.-C. Lai, S.-H. Chiu, *Angew. Chem. Int. Ed.* **2008**, *47*, 4436-4439.
[40] A. López-Moreno, E. M. Perez, *Chem. Comm.* **2015**, *51*, 5421-5424.

[41] J. Villalva, A. Rapakousiou, M. A. Monclús, J. P. Fernández Blázquez, J. de la Vega, A. Naranjo, M. Vera-Hidalgo, M. L. Ruiz-González, H. Pedersen, E. M. Pérez, *ACS Nano* **2023**, *17*, 16565-16572.
[42] F. L. Sebastian, N. F. Zorn, S. Settele, S. Lindenthal, F. J. Berger, C. Bendel, H. Li, B. S. Flavel, J. Zaumseil, *J. Phys. Chem. Lett.* **2022**, *13*, 3542-3548.
[43] E. Martínez-Perinan, A. de Juan, Y. Pouillon, C. Schierl, V. Strauss, N. Martín, A. Rubio, D. M. Guldi, E. Lorenzo, E. M. Pérez, *Nanoscale* **2016**, *8*, 9254-9264.
[44] A. V. Naumov, S. Ghosh, D. A. Tsyboulski, S. M. Bachilo, R. B. Weisman, *ACS Nano* **2011**, *5*, 1639-1648.
[45] N. R. Raravikar, P. Keblinski, A. M. Rao, M. S. Dresselhaus, L. S. Schadler, P. M. Ajayan, *Phys. Rev. B* **2002**, *66*, 235424.
[46] Y. Pan, D. Baster, D. Käch, J. Reger, L. Wettstein, F. Krumeich, M. El Kazzi, M. J. Bezdek, *Angew. Chem. Int. Ed.*, **2024**, *63*, e202412084.

## Data availability statement

The authors declare that all the data that support these findings are available in the manuscript, including its supporting information. Information files and from the corresponding authors upon request. Source data are provided with this paper.